Fokker-Planck Simulation Study of Alfvén Eigenmode Bursts

Y. Todo, T.-H. Watanabe, Hyoung-Bin Park[1], and T. Sato

Theory and Computer Simulation Center,
National Institute for Fusion Science, 322-6 Oroshi-cho, Toki-shi 509-5292, Japan

e-mail contact of main author: todo@nifs.ac.jp

Abstract. Recurrent bursts of toroidicity-induced Alfvén eigenmodes (TAEs) are reproduced with a Fokker-Planck-magnetohydrodynamic simulation where a fast-ion source and slowing down are incorporated self-consistently. The bursts take place at regular time intervals and the behaviors of all the TAEs are synchronized. The fast-ion transport due to TAE activity spatially broadens the classical fast-ion distribution and significantly reduces its peak value. Only a small change of the distribution takes place with each burst, leading to loss of a small fraction of the fast ions. The system stays close to the marginal stability state established through the interplay of the fast-ion source, slowing down, and TAE activity.

1. Introduction

The toroidicity-induced Alfvén eigenmode (TAE) is a shear-Alfvén eigenmode in toroidal plasmas [1]. TAEs can be destabilized by fast ions which have velocities comparable to the Alfvén velocity. Several years ago, recurrent bursts of TAEs were observed with drops in neutron emission during neutral beam injection in TFTR [2] and DIII-D [3]. The drops in neutron emission have been recognized as a manifestation of TAE-induced fast-ion loss. Nonlinear evolution of TAEs, especially the TAE bursts, is an important issue for fusion reactors, since successful confinement of energetic alpha particles is required for self-sustained operation. It must be noted that multiple TAEs are destabilized during TAE bursts and bursts take place at regular time intervals. The fraction of the drop in neutron emission to the total emission in TFTR plasmas was typically less than 10% (Fig. 4 of Ref. [2]).

It was demonstrated with numerical simulation of a system reduced by a mapping method that the resonance overlap of multiple TAEs enhances the energy release from fast ions to TAEs and synchronizes the behavior of multiple TAEs [4]. More realistic simulations which incorporate the TAE mode structure and the resonance conditions in a realistic tokamak are needed to make more quantitative comparisons with experiment. Recently, Candy *et al.* [5] carried out δf particle simulation where linear eigenmodes are coupled with fast-ion dynamics and reproduced a bursting behavior of TAEs with realistic plasma parameters. In Ref. [5] a single dominant TAE which grows up to an amplitude of $\delta B/B \sim 2 \times 10^{-2}$ creates orbit islands in the phase space. Overlap of orbit islands makes the entire phase space stochastic and allows rapid conversion of particle free energy to wave energy. The large stochastic region causes a complete flattening of the fast-ion density profile. Although this is one possible mechanism of periodic bursts due to neutral beam injection, it seems unlikely for TFTR and DIII-D experiments since multiple modes were observed.

Another simulation method, namely Fokker-Planck-magnetohydrodynamic (MHD) simulation, has been developed [6, 7, 8]. Results of the Fokker-Planck-MHD simulation have shown that TAE bursts take place if the fast-ion slowing-down time is sufficiently longer than the TAE

[1]Present address: Samsung Advanced Institute of Technology, P.O. Box 111, Suwon 440-600, Korea.

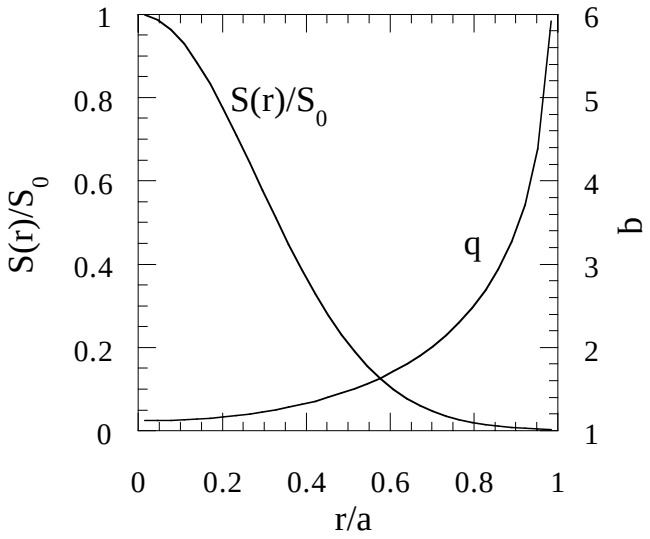

FIG. 1. The fast-ion source profile and the q-profile as functions of the minor radius.

damping time and the heating power is sufficiently high. In this paper we report new simulation results where a few percent of fast ions are lost with each TAE burst and all the TAEs have a synchronized behavior. We analyze the time evolution of the fast-ion distribution and show that the change of distribution with each burst is relatively small compared with the distribution itself.

2. Simulation Model

A kinetic-MHD hybrid simulation model, which was used to investigate the saturation mechanism of collisionless fast-ion driven TAEs [9, 10], is employed. In this model the plasma is divided into two parts, the background plasma and fast ions. The background plasma is described by the nonlinear full MHD equations and the electromagnetic field is given by the MHD description. This approximation is reasonable under the condition that the fast-ion density is much less than the background plasma density. The MHD equations are,

$$\frac{\partial \rho}{\partial t} = -\nabla \cdot (\rho \mathbf{v}), \tag{1}$$

$$\rho \frac{\partial}{\partial t}\mathbf{v} + \rho \mathbf{v} \cdot \nabla \mathbf{v} = -\nabla p + \frac{1}{\mu_0}(\nabla \times \mathbf{B}) \times \mathbf{B} + \nu \rho \triangle \mathbf{v}, \tag{2}$$

$$\frac{\partial \mathbf{B}}{\partial t} = -\nabla \times \mathbf{E}, \tag{3}$$

$$\frac{\partial p}{\partial t} = -\nabla \cdot (p\mathbf{v}) - (\gamma - 1) p \nabla \cdot \mathbf{v}, \tag{4}$$

$$\mathbf{E} = -\mathbf{v} \times \mathbf{B}, \tag{5}$$

where μ_0 is the vacuum magnetic permeability and γ is the adiabatic constant, and all other quantities are conventional.

We use a four-dimensional phase space (R, φ, z, v), where v is the parallel velocity and (R, φ, z) are the cylindrical coordinates. Only the parallel velocity component is taken into account for simplicity. However, we adopt a Jacobian for the three-dimensional velocity space to be consistent with the slowing-down term. The grid numbers used are $(65, 72, 65, 20)$ for (R, φ, z, v)

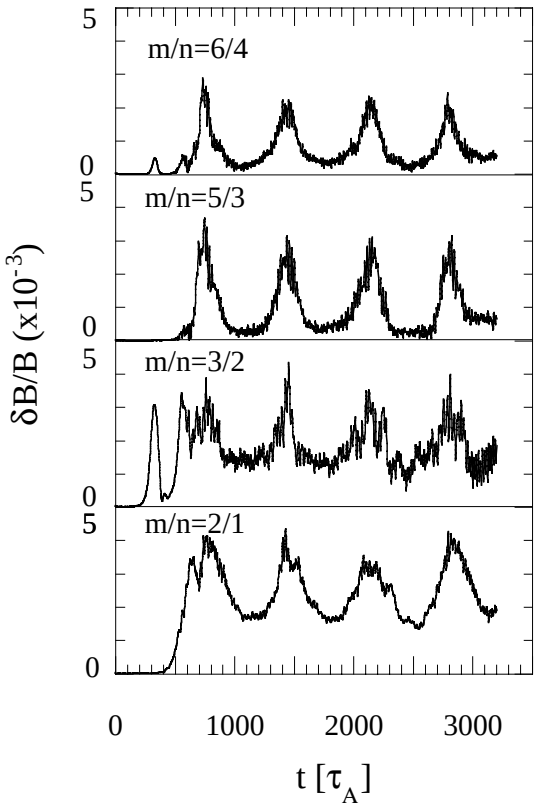

FIG. 2. Time evolutions of radial magnetic field fluctuations of $m/n = 2/1, 3/2, 5/3$, and $6/4$ harmonics.

coordinates, respectively. The initial condition is an MHD equilibrium where the aspect ratio is 3. For analysis of simulation data a flux coordinate system (r, φ, θ) is constructed. The unit of length is the Larmor radius of a fast ion whose velocity is equal to the Alfvén velocity ($\equiv v_A m_f/q_f B$) at the initial magnetic axis. The minor radius denoted as a is taken to be 16, and the simulation domain is ($32 \leq R \leq 64$, $0 \leq z \leq 32$). The initial magnetic axis locates at $(R = R_0 \equiv 50.5, z = z_0 \equiv 16)$. The unit of time is the Alfvén time ($\tau_A \equiv R_0/v_A$).

The effect of fast ions on the MHD fluid is taken into account in the MHD momentum equation through the fast-ion perpendicular current [10, 11]. The time evolution of the fast-ion distribution is described by the following Fokker-Planck equation:

$$\begin{aligned}
\frac{\partial}{\partial t} f &= -\nabla \cdot (\mathbf{v}_D) - \frac{\partial}{v^2 \partial v} v^2 a_H f \\
&+ \frac{1}{\tau_s} \frac{\partial}{v^2 \partial v} (v_{\rm crit}^3 + v^3) f + \frac{S(\mathbf{x})}{v^2} \delta(v - v_0), \qquad (6) \\
\mathbf{v}_D &= \frac{v}{B} \left[\mathbf{B} + \frac{m_f}{q_f} v \nabla \times \mathbf{b} \right] + \frac{1}{B} [\mathbf{E} \times \mathbf{b}], \qquad (7) \\
\mathbf{b} &= \mathbf{B}/B, \qquad (8) \\
a_H &= \frac{v}{B} \nabla \times \mathbf{b} \cdot \mathbf{E}, \qquad (9) \\
S(\mathbf{x}) &= S_0 \exp\{-\alpha^2 [(R - R_0)^2 + (z - z_0)^2]\} \, . \qquad (10)
\end{aligned}$$

Here, $v_{\rm crit}$ is the critical velocity above which collisions with background electrons dominate over those with background ions, and v_0 is the birth velocity of fast ions. We choose $v_{\rm crit} =$

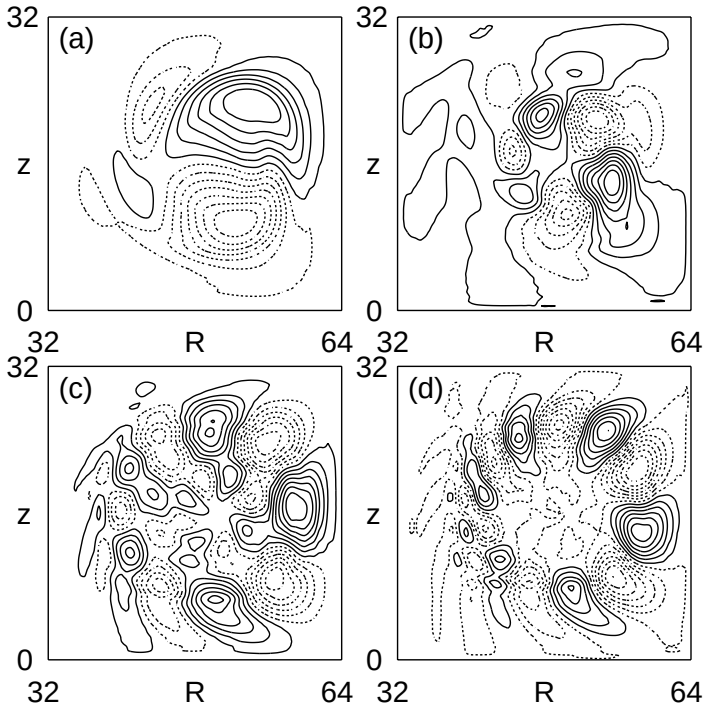

FIG. 3. Contours of the toroidal electric field on a poloidal cross-section at $t = 713\tau_A$ for toroidal mode numbers of (a) $n = 1$, (b) $n = 2$, (c) $n = 3$, and (d) $n = 4$.

$0.3v_A$ and $v_0 = 1.5v_A$, respectively. On the right-hand side of Eq. (6), the slowing-down time is denoted as τ_s and chosen $\tau_s = 2000\tau_A$. The fourth term of Eq. (6) represents the source of fast ions. In Eq. (10) α is set to be equal to $1/0.4a$, and S_0 is chosen so that the central fast-ion beta value of the classical distribution is 2%. The classical distribution is realized through a balance between the source and the slowing down and is a steady solution without any nonaxisymmetric modes, especially TAE activities. The source profile is shown in Fig. 1 with the q-profile. A finite viscosity of $2 \times 10^{-5} v_A R_0$ is considered to mimic the damping of TAEs. It yields, for example, an e-folding damping time of $130\tau_A$ for an $n = 2$ TAE, which is the most unstable TAE in the simulation described below. The Fokker-Planck equation and the full MHD equations are solved with a finite difference method of a fourth-order accuracy in space and time.

3. Results

Time evolutions of radial magnetic fluctuation harmonics in the simulation results are shown in Fig. 2. Four TAEs with the toroidal mode numbers from 1 to 4 are destabilized. Figure 3 shows contours of the toroidal electric field of the four TAEs on a poloidal cross-section at $t = 713$. The frequencies of $m/n = 2/1, 3/2, 5/3$, and $6/4$ harmonics are $0.28\omega_A$, $0.35\omega_A$, $0.28\omega_A$, and $0.30\omega_A$, respectively, and these are reasonable values for TAEs. At $t = 0$ there are no fast ions and as time passes fast ions gradually accumulate due to the fast-ion source. Accumulated fast ions destabilize the $n = 2$ TAE first at $t = 300$. Later than this precursory growth of the $n = 2$ TAE, the other TAEs grow up to levels comparable to that of the $n = 2$ TAE and the behaviors of all the TAEs are synchronized.

We turn to the detailed behavior of the burst. In Fig. 4 we show time evolutions of the total TAE energy and the peak value of the fast-ion distribution function at $v = v_A$. We can see a

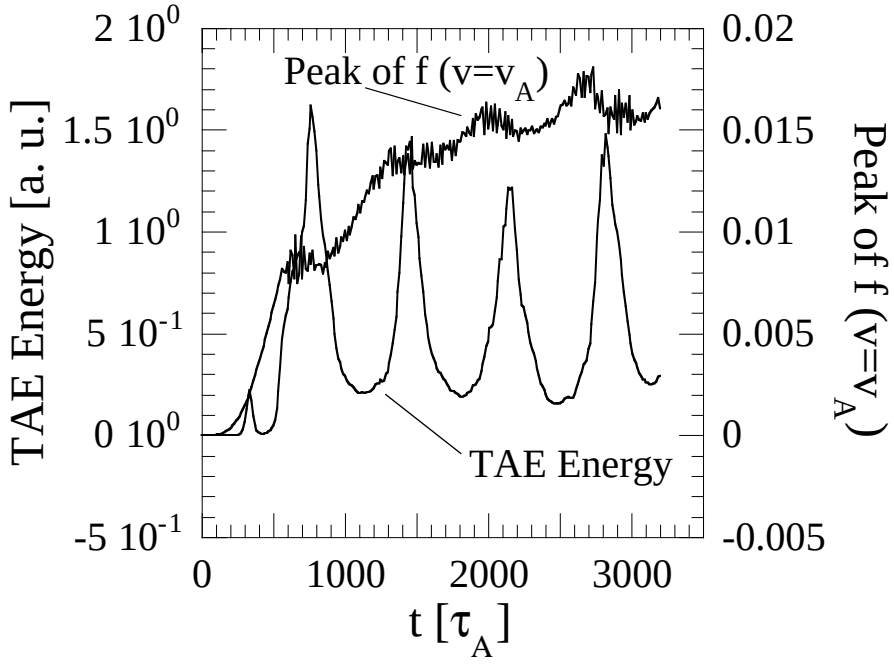

FIG. 4. Time evolutions of total TAE energy and the fast-ion distribution peak value for $v = v_A$.

correlation between the drop in fast-ion distribution and the growth of TAE energy. Figure 5 shows as a bird's-eye view plot in (t, R) space the time evolution of the fast-ion distribution averaged in the toroidal angle with $v = v_A$ on the midplane. The bright parts are regions flattened due to TAE activity. TAEs flatten the fast-ion spatial distribution through the $\mathbf{E} \times \mathbf{B}$ trapping. In contrast to the bright flattened regions, we can see dark regions elongated in the R-direction around $t = 700, 1400, 2100$, and 2800 accompanying the TAE bursts. These dark regions are rapid temporal changes of the fast-ion distribution. For greater clarity, the fast-ion distributions are plotted in Fig. 6 as functions of the major radius (a) at $t = 2000$ (before the burst) and (b) at $t = 2300$ (after the burst) with the classical distribution, which is a steady solution obtained with a simulation suppressing any nonaxisymmetric modes, especially TAE activities. Comparing the distributions before and after the burst, it can be seen that the fast ions are transported outwards across a distribution precipice at $R = 59$. We must pay attention to the following: (1) compared with the classical distribution, the two distributions before and after the burst are significantly broadened in the radial direction and their peak values are also reduced by half, (2) the change of the distribution function during the burst is relatively small compared with the distribution itself. The former means that the fast-ion distribution is significantly affected by the TAE activity. The latter indicates that the difference between the unstable state (before the burst) and the stable state (after the burst) is small. Thus, we conclude that the system stays close to the marginal stability state which is established through the interplay of the fast-ion source, slowing down, and multiple TAE activity. This is a behavior different from that found in the particle simulation [5] where with each burst the fast ion density is completely flattened from a steep-gradient state.

We show the time evolutions of total fast-ion energy and total TAE energy in Fig. 7. It can be seen that drops in fast-ion energy of 3% take place accompanying TAE bursts. These drops are due to fast-ion loss and are similar to those in neutron emission in neutral-beam-injected plasmas [2, 3]. The fast-ion loss is a result of the outward transport of fast ions.

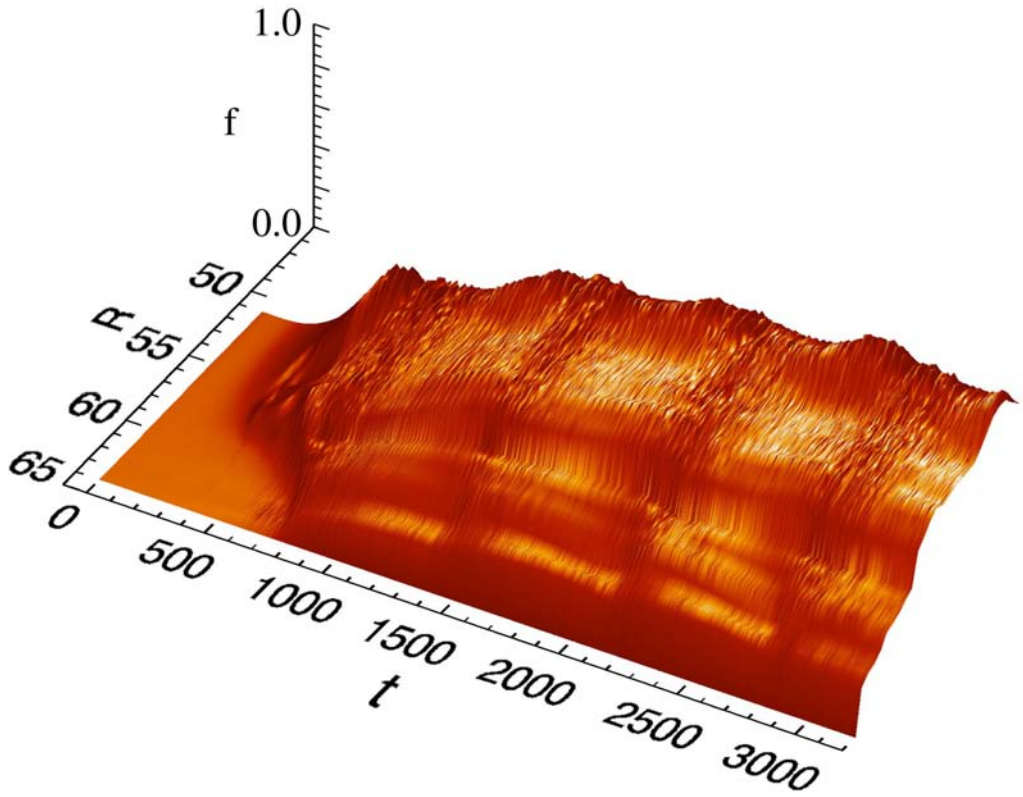

FIG. 5. Bird's-eye view plot of the time evolution of the fast-ion distribution on the (t, R) plane. The distribution is averaged in toroidal angle on the midplane $(z = 16)$ at $v = v_A$.

4. Discussion and Summary

TAE bursts with loss of a small fraction of fast ions have been discussed in the resonance overlap scenario of multiple modes [12]. The synchronization of multiple TAEs in the present simulation results is consistent with the resonance overlap scenario [4]. The bursting behavior of TAEs has been explained by the simple predator-prey model [13]. However, the model cannot explain many characteristics revealed in the present simulation such as the synchronization of multiple TAEs and the spatial broadening of the fast-ion distribution. Furthermore, we would like to emphasize that the present simulation is based on fundamental physics principles.

Finally, let us compare the simulation and experimental results. If we apply the parameters $B_0 = 1$ [T], $R_0 = 2.4$ [m], and $n_0 = 3 \times 10^{19}$ [m^{-3}], which are typical for the TAE bursts in the TFTR deuterium plasma [2], the bursting period of 700 τ_A in the simulation results corresponds to 0.6 [ms]. This is shorter than the typical experimental value of 2 [ms]. This discrepancy arises from the fact that the heating time scale, which we define as the ratio of the accumulated fast-ion energy to the heating power, is shorter in the present simulation than in the typical TFTR experiment by a factor of 7. The simulation time step is limited by the time for the MHD fast mode to propagate the grid size, whereas we must simulate a time span of the several burst periods which is roughly comparable to the heating time scale. Our purpose in employing such a short heating time scale is to reduce the time span simulated and make the CPU time reasonable. Nevertheless, even on the present simulation run we have spent 70 hours using 15 CPU of NEC SX-4/64M2. The short burst period in the simulation results also leads to the

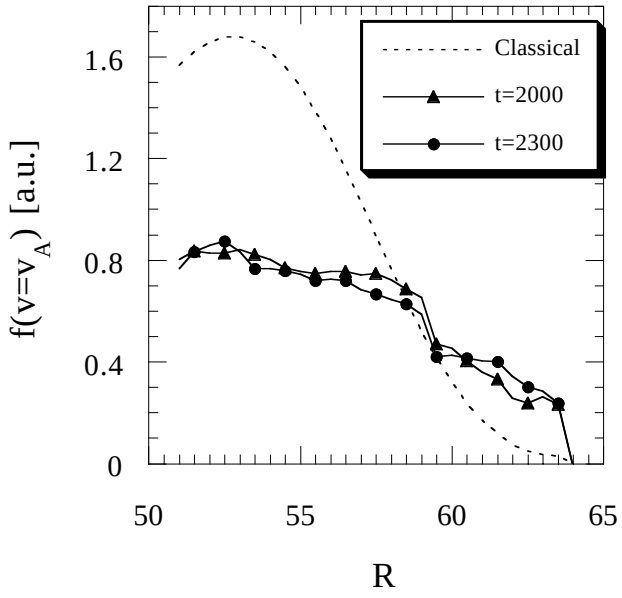

FIG. 6. Fast-ion distributions before $(t = 2000)$ and after $(t = 2300)$ the TAE burst and the classical distribution, as functions of the major radius.

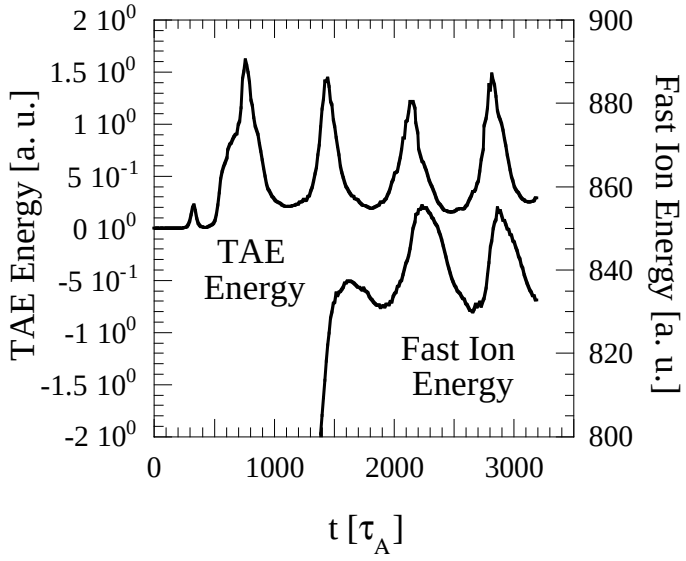

FIG. 7. Time evolutions of total TAE energy and fast-ion energy.

small ratio of the maximum amplitude to the minimum amplitude of $n = 1$ and 2 TAEs, since these modes do not have enough time to damp in the short quiescent period. Therefore, more realistic simulation is needed to make more strict comparison. We must note, however, that the volume-averaged fast-ion beta value at the end of the simulation is 0.6% which is comparable to the experiment. Since the fast-ion beta value is crucial for the TAE evolution, we have chosen the slowing-down time and the source intensity S_0 to meet the fast-ion beta with experiment.

In conclusion, we have successfully reproduced the recurrent TAE bursts and TAE-induced fast-ion loss with the Fokker-Planck-MHD simulation. The TAE bursts take place at regular time intervals and the behaviors of all the TAEs are synchronized. The fast-ion transport due to TAE activity spatially broadens the classical fast-ion distribution and significantly reduces its peak value. Only a small change of the distribution takes place with each burst, leading to loss of a small fraction of fast ions. The synchronization of multiple TAEs and the loss of small fraction of fast ions are consistent with the resonance overlap scenario. The system stays close to the marginal stability state established through the interplay of fast-ion source, slowing down, and TAE activity.

ACKNOWLEDGMENTS

Numerical computations were performed at the Man-Machine Interactive System for Simulation (MISSION) of National Institute for Fusion Science. This work was partially supported by Grant-in-Aid of the Ministry of Education, Science, Sports, and Culture (No. 11780363).

References

[1] C. Z. Cheng and M. S. Chance, Phys.Fluids **29**, 3659 (1986).

[2] K. L. Wong *et al.*, Phys. Rev. Lett. **66**, 1874 (1991).

[3] H. H. Duong *et al.*, Nucl. Fusion **33**, 749 (1993).

[4] H. L. Berk, B. N. Breizman, and M. S. Pekker, Nucl. Fusion **35**, 1713 (1995).

[5] J. Candy *et al.*, Phys. Plasmas **6**, 1822 (1999).

[6] Y. Todo and T. Sato, in *Theory of Fusion Plasmas, 1998*, Varenna (Società Italiana di Fisica, Bologna, 1999), p. 229.

[7] Y. Todo and T. Sato, in *Fusion Energy, 1998*, Yokohama (International Atomic Energy Agency, Vienna, 1999), Vol. 4, p. 1577.

[8] Y. Todo and T. Sato, J. Plasma Fusion Res. SERIES **2**, 263 (1999).

[9] G. Y. Fu and W. Park, Phys. Rev. Lett. **74**, 1594 (1995).

[10] Y. Todo *et al.*, Phys. Plasmas **2**, 2711 (1995).

[11] Y. Todo and T. Sato, Phys. Plasmas **5**, 1321 (1998)

[12] H. L. Berk and B. N. Breizman, in *Theory of Fusion Plasmas, 1998*, Varenna (Società Italiana di Fisica, Bologna, 1999), p. 283.

[13] W. W. Heidbrink *et al.*, Phys. Fluids B **5**, 2176 (1993).